


Science

AAAS

**Increased Compressibility of Pseudobrookite-Type
MgTi 2O5 Caused by Cation Disorder**Robert M. Hazen, *et al.**Science* **277**, 1965 (1997);

DOI: 10.1126/science.277.5334.1965

**The following resources related to this article are available online at
www.sciencemag.org (this information is current as of November 19, 2007):**

Updated information and services, including high-resolution figures, can be found in the online version of this article at:

<http://www.sciencemag.org/cgi/content/full/277/5334/1965>

This article **cites 10 articles**, 5 of which can be accessed for free:

<http://www.sciencemag.org/cgi/content/full/277/5334/1965#otherarticles>

This article has been **cited by** 19 article(s) on the ISI Web of Science.

This article has been **cited by** 1 articles hosted by HighWire Press; see:

<http://www.sciencemag.org/cgi/content/full/277/5334/1965#otherarticles>

This article appears in the following **subject collections**:

Geochemistry, Geophysics

http://www.sciencemag.org/cgi/collection/geochem_phys

Information about obtaining **reprints** of this article or about obtaining **permission to reproduce this article** in whole or in part can be found at:

<http://www.sciencemag.org/about/permissions.dtl>

Downloaded from www.sciencemag.org on November 19, 2007

imum for solar cycle 22 during 1996, then the ACRIM mean TSI was $0.0361 \pm 0.0006\%$ higher for the current minimum than for cycle 21 (Table 2 and Fig. 2). Degradation corrections for the ACRIM experiments are uncertain by less than $\pm 0.005\%$ per decade (4). The total root-mean-square uncertainty of the trend is also less than $\pm 0.005\%$, which indicates that the difference in ACRIM TSI between the solar minima in 1986 and 1996 is well resolved.

Similarly, the corresponding mean ERBS results changed by $0.0271 \pm 0.0036\%$ between 1986 and 1996 (Fig. 2). The ERBS uncertainty does not include sensor degradation, and significant changes of ERBS results can be observed in the record when no comparable signals are present in other TSI data (Figs. 1 and 2). Accelerated degradation during the rising activity phase of solar cycle 22 is likely, with an amplitude ranging up to the shift in the ERB/ERBS ratio ($\sim 0.03\%$). The ERBS trend is corroborative, but its degradation uncertainty limits it to qualitative interpretations.

The TSI trend is significant for direct solar climate forcing. The response of climate to TSI variation is complex, but a sensitivity is predicted by global circulation models at ~ 1 K per 1% change in TSI (18). If sustained, the ACRIM TSI trend is near that required to produce, on 200-year time scales, a climate change comparable to (but in the opposite sense of) the estimated 0.4 to 1.5 K average temperature decrease during the Little Ice Age climate anomaly (3, 19). The climatic effect of greenhouse warming over the next 50 to 100 years is estimated to be 1.5 to 4.5 K (19). By comparison, the TSI trend could produce additional warming of ~ 0.4 K in 100 years, a potentially significant contribution.

REFERENCES AND NOTES

1. R. C. Willson, in *The Sun as a Variable Star, International Astronomical Union Colloquium 143 Proceedings*, J. Pap, C. Fröhlich, H. Hudson, K. Solanki, Eds. (Cambridge Univ. Press, New York, 1994), pp. 54–62.
2. J. A. Eddy, *Science* **192**, 1189 (1976).
3. P. E. Damon and C. P. Sonett, in *The Sun in Time*, C. P. Sonett, M. S. Giampapa, M. S. Mathews, Eds. (Univ. of Arizona Press, Tucson, AZ, 1991), pp. 360–388.
4. R. C. Willson and H. S. Hudson, *Nature* **351**, 42 (1991).
5. D. Hoyt and L. Kyle, in *Proc. Climate Impact of Solar Variability* (NASA Conf. Rep. 3086, NASA, Greenbelt, MD, 1990), pp. 293–300.
6. R. B. Lee III, M. A. Gibson, R. S. Wilson, S. Thomas, *J. Geophys. Res.* **100**, 1667 (1995).
7. R. C. Willson and H. S. Hudson, *Nature* **332**, 810 (1988).
8. ACRIM II results are reported on the ACRIM I scale using the ACRIM I/ACRIM II ratio (1.001689) derived in the text.
9. R. C. Willson, S. Gulkis, M. Janssen, H. S. Hudson, G. A. Chapman, *Science* **211**, 700 (1981).
10. The ERB and ERBS experiments view the sun as it passes through their fields of view for only a few

minutes per orbit, whereas the ACRIM experiments are solar-pointed for at least 10 shutter cycles per orbit, every orbit, every day. During most of the ERB mission, observations were made every orbit on 3 of every 4 days. The ERBS experiments observe the sun for a few minutes during one orbit every 2 weeks.

11. UV irradiances, their surrogates (Hel 1083 and F10.7 cm fluxes), and the Zurich sunspot number were at a minimum in mid-1996. ACRIM II results showed a local minimum near the same time. The broad TSI minimum of solar cycle 21 was centered about 6 months before solar minimum, as defined by reversal of active-region magnetic polarity in September 1986. Definition of the actual location of the cycle 22 TSI minimum must await analysis of the 1997 ACRIM II results.
12. H. L. Kyle, D. V. Hoyt, J. R. Hickey, B. J. Vallette, *Nimbus-7 Earth Radiation Budget Calibration History—Part I: The Solar Channels* (NASA Ref. Pub. 1316, NASA, Greenbelt, MD, 1993), p. 27.
13. A. T. Mecherikunnel, *Sol. Phys.* **155**, 211 (1994).
14. H. L. Kyle et al., *Nimbus-7 Earth Radiation Budget Compact Solar Data Set User's Guide* (NASA Ref. Pub. 1346, NASA, Greenbelt, MD, 1994).
15. Degradation of the cavity sensors of TSI experiments is a phenomenon that usually occurs in two phases. The first is rapid degradation that occurs when the cavity's solar flux-absorbing surface is modified by its initial exposure to space and the radiation environment. The sensors then settle into a "mission" degradation modality as further exposure to solar flux slowly alters the cavity's absorbing surfaces. The

rates of initial and mission degradation vary between experiments, but the degradation phenomena are common to most of them. It was further observed in the ACRIM I experiment that the rate of degradation was proportional to both the amount of solar exposure and the relative abundance of high energy, short-wavelength flux. During periods of intense solar magnetic activity, the enhanced amounts of high-energy, short-wavelength solar radiation increase the rate of degradation.

16. A lower susceptibility for ERB to accelerated degradation would be expected because of its longer history of solar exposure, including the peak activity period of solar cycle 21. Its sensor surfaces may have been near their degradation saturation point during solar cycle 22.
17. R. C. Willson, paper presented at American Geophysical Union meeting, Baltimore, MD, May 1997.
18. D. Rind and J. Overpeck, *Quat. Sci. Rev.* **12**, 347 (1993).
19. National Research Council, *Solar Influences on Global Change* (National Academy Press, Washington, DC, 1994), pp. 36–40.
20. I thank J. Hansen, L. Kyle, A. Mecherikunnel, R. Lee III, and R. Wilson for providing helpful discussions, documentation, data, and advice. The ACRIM II experiment is supported by NASA at Columbia University under NASA contract NAS5-97164. The ACRIM II results are available from the NASA Goddard Space Flight Center and Langley Research Center Distributed Active Archive Centers.

18 June 1997; accepted 15 August 1997

Increased Compressibility of Pseudobrookite-Type MgTi_2O_5 Caused by Cation Disorder

Robert M. Hazen* and Hexiong Yang

Compressibilities were determined for four pseudobrookite-type magnesium titanate (MgTi_2O_5) samples with different degrees of Mg-Ti disorder. Compressibilities of *a* and *c* axes in disordered MgTi_2O_5 were 10% and 7% greater, respectively, than those of a relatively ordered sample. The estimated bulk moduli for fully ordered and disordered MgTi_2O_5 are 167 ± 1 and 158 ± 1 gigapascals, respectively. This difference is an order of magnitude greater than that predicted by bulk modulus–volume systematics. Cation order, in addition to composition and structure information, is thus important when documenting the elasticity of crystalline phases. Elastic constants of mantle silicates that are subject to pressure-induced cation ordering must be reevaluated.

Pressure-volume equations of state (EOS) of crystalline solids impose important constraints on models of interatomic bonding, and they provide an essential foundation for interpreting seismic data from Earth's deep interior. Conventional wisdom suggests that EOS are principally dependent on only two variables: structure and composition. Summaries of mineral EOS parameters (1), for example, are tabulated according to these two variables. Details on the state of order-disorder—which may be important in characterizing the thermochemistry and

transport properties of minerals as well as those of alloys, ceramics, and other crystalline phases—are usually omitted in discussions of EOS. Recent studies demonstrate that order-disorder phenomena may be affected by pressure in phases that display a nonzero volume of disordering $\Delta V_{\text{dis}} = V_{\text{disordered}} - V_{\text{ordered}}$ (2). Silicate minerals commonly display ΔV_{dis} up to 0.5% (3, 4), and values exceeding 1% have been observed in oxides and sulfides (5). However, the extent to which differing states of order affect the physical properties of phases at high pressure is not known.

The comparative compressibility technique, in which several crystals are mounted in the same diamond-anvil cell experiment, can be used to discern subtle differ-

Geophysical Laboratory and Center for High Pressure Research, Carnegie Institution of Washington, 5251 Broad Branch Road NW, Washington, DC 20015, USA.

*To whom correspondence should be addressed. E-mail: hazen@gl.ciw.edu

ences in EOS. This method has been used, for example, to document otherwise unresolvable differences in the bulk moduli of wüstites with different degrees of oxygen deficiency (6), nonstoichiometric omphacitic pyroxenes (7), Fe-Mg wadsleyites (8), silicate spinels (9), and majoritic garnets (10). Here, we examined EOS of pseudobrookite-type MgTi_2O_5 (karrooite), a dense oxide that displays a wide range of ordered states (11).

Four synthetic MgTi_2O_5 crystals were annealed at 600°, 700°, 1000°, and 1400°C. Single-crystal x-ray diffraction techniques were used to characterize the orthorhombic (space group $Bbmm$) unit-cell parameters and to determine the crystal structure and ordered

state of each sample (Table 1). Ambient-pressure unit-cell parameters for the most ordered crystal of this study are $a = 9.712 \text{ \AA}$, $b = 10.019 \text{ \AA}$, $c = 3.736 \text{ \AA}$, volume = 363.52 \AA^3 ; those for the most disordered crystal are $a = 9.760 \text{ \AA}$, $b = 9.979 \text{ \AA}$, $c = 3.748 \text{ \AA}$, volume = 365.00 \AA^3 . The ordered form of MgTi_2O_5 is denser than the disordered form—a commonly observed situation for close-packed oxide and silicate phases (2). These observed unit-cell parameters can be used to estimate ambient-pressure unit-cell volumes for fully ordered and fully disordered MgTi_2O_5 (Table 1). Estimated volumes for ordered and disordered end members are 363.2 and 365.3 \AA^3 , respectively—a 0.6% difference. Bulk modulus–volume systematics (12), which document an inverse relation between unit-cell volume and bulk modulus (K) of isostructural compounds, thus predict that disordered MgTi_2O_5 should be about 0.6% more compressible than the ordered variant.

Pseudobrookite has two nonequivalent, octahedrally coordinated cation sites, denoted M1 and M2; each formula unit has one M1 and two M2 sites. In fully disordered MgTi_2O_5 the average compositions of both M1 and M2 are $(\text{Mg}_{0.33}\text{Ti}_{0.67})$. Our most disordered crystal, which was rapidly quenched from 1400°C after annealing for 5 hours, has the formula $(\text{Mg}_{0.515}\text{Ti}_{0.485})(\text{Ti}_{0.758}\text{Mg}_{0.242})_2\text{O}_5$. In our

most ordered crystal, annealed at 600°C for 35 days, the composition is $(\text{Mg}_{0.93}\text{Ti}_{0.07})(\text{Ti}_{0.965}\text{Mg}_{0.035})_2\text{O}_5$. The four crystals (Table 1) thus represent a wide range of Mg-Ti ordered states. These four ordered variants were mounted in one diamond-anvil cell (9). Unit-cell parameters for all four crystals were determined at 13 pressures, and x-ray intensity data were collected for the most ordered and disordered samples at seven pressures to 7.51 GPa (13).

The b -axis compressibility (Fig. 1) is about 0.0024 GPa^{-1} for all four ordered variants, but the compressibilities of the a and c axes in disordered MgTi_2O_5 are 10% and 7% greater, respectively, than corresponding values for the ordered phase. Axial compression ratios thus vary from 1.58:2.02:1.00 for the most ordered crystal to 1.63:1.85:1.00 for the most disordered crystal. Resulting K values for these two MgTi_2O_5 crystals (assuming the pressure derivative of K , $K' = 4$) are 166.8 ± 0.9 and $160.2 \pm 0.7 \text{ GPa}$, respectively—a 4% difference (Fig. 2). Intermediate Mg-Ti ordered states display intermediate K (Table 1 and Fig. 3). We extrapolate K for fully ordered and fully disordered MgTi_2O_5 to be 167.3 ± 1.0 and $157.6 \pm 1.0 \text{ GPa}$ —a 6%

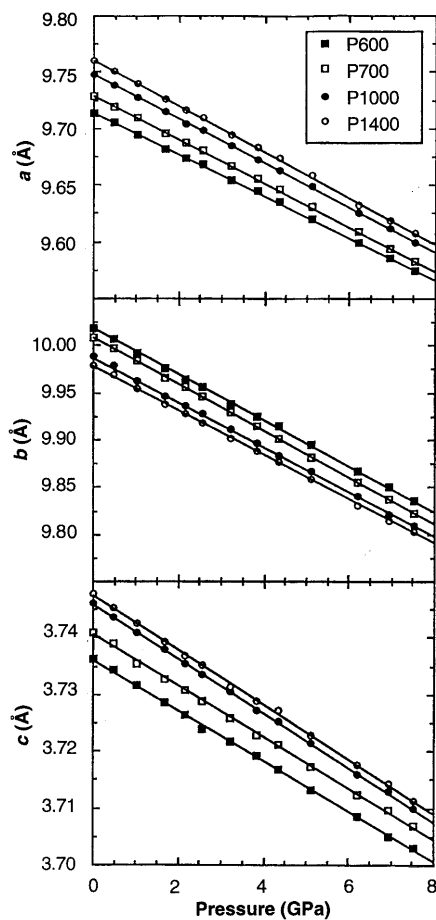


Fig. 1. Variations of unit-cell dimensions for four ordered variants of MgTi_2O_5 . The b axis displays similar compressibility (that is, the four lines of b versus pressure are essentially parallel). This behavior contrasts with that of the a and c axes; axes of the disordered end member are more compressible by 10% and 7%, respectively, relative to the more ordered variant. The almost fully ordered specimen P600 was annealed at 600°C for 35 days, the relatively disordered specimen P1400 was quenched rapidly from 1400°C, and specimens P700 and P1000 with intermediate states of order were annealed at 700° and 1000°C, respectively.

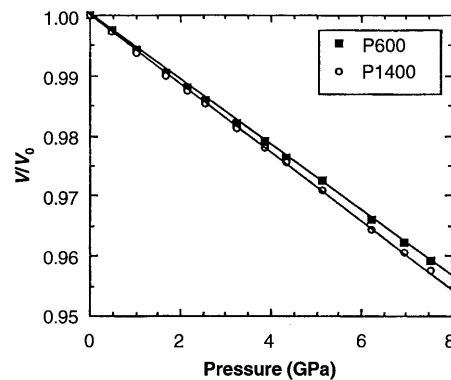


Fig. 2. Relative volume (V/V_0) for MgTi_2O_5 crystals versus pressure. The partially disordered specimen P1400 is about 5% more compressible than the almost fully ordered specimen P600.

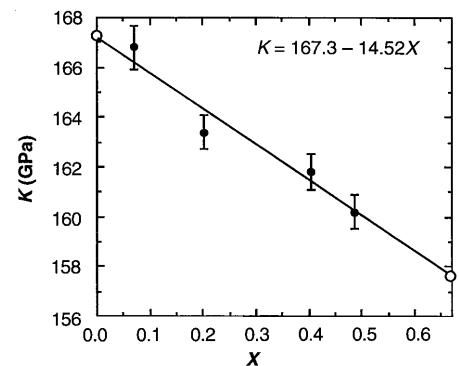


Fig. 3. Observed isothermal bulk modulus K (assuming $K' = 4$) for four MgTi_2O_5 crystals versus disorder parameter X . Extrapolated bulk moduli for fully ordered ($X = 0$) and fully disordered ($X = 0.67$) MgTi_2O_5 are 167.3 ± 1.0 and $157.6 \pm 1.0 \text{ GPa}$, respectively.

Table 1. Observed ambient-pressure unit-cell parameters, refined octahedral cation occupancies, and isothermal bulk moduli (assuming $K' = 4$) for four samples of MgTi_2O_5 , and estimated values for fully ordered and disordered end members. Ideal values are extrapolated from observed unit-cell parameters and bulk moduli in this table. Numbers in parentheses are estimated errors in terms of last significant digits.

T (°C)	a (Å)	b (Å)	c (Å)	V (Å ³)	X^*	K (GPa)
Ideal (ordered)	9.7031	10.0262	3.7329	363.17	0	167.3
600	9.7115(5)	10.0189(3)	3.7362(2)	363.52(3)	0.070(5)	166.8(9)
700	9.7264(3)	10.0092(3)	3.7409(2)	364.19(3)	0.203(3)	163.4(7)
1000	9.7461(6)	9.9875(4)	3.7464(4)	364.67(4)	0.404(5)	161.8(7)
1400	9.7597(4)	9.9789(4)	3.7478(3)	365.00(3)	0.485(5)	160.2(7)
Ideal (disordered)	9.7785	9.9638	3.7495	365.32	0.667	157.6

*Ti in M1 = X ; Mg in M1 = $1 - X$; Ti in M2 = $1 - X/2$; Mg in M2 = $X/2$.

difference, which is an order of magnitude greater than that predicted by K - V systematics. This unexpected 6% change is greater than the variations in K observed for the entire compositional range of Mg-Fe solid solution in many oxides and silicates (2).

The observed dependence of K on Mg-Ti ordering is a consequence of the differential compressibilities of weaker $\text{Mg}^{2+}\text{-O}$ and stronger $\text{Ti}^{4+}\text{-O}$ bonds. The structure parallel to the b axis features an alternating sequence of one M1 and two M2 octahedra. Compressibility along this direction, therefore, is always the average of one Mg-O and two Ti-O bonds, regardless of the state of Mg-Ti order. Compression along the a and c axes, by contrast, is dictated primarily by M2 octahedra, which form a continuous edge-sharing octahedral linkage in the (010) plane. In ordered MgTi_2O_5 , the M1 (Mg) octahedron is relatively compressible with an octahedral K of 172 ± 4 GPa, whereas the M2 (Ti) octahedron is relatively rigid with an octahedral K of 250 ± 7 GPa. In disordered MgTi_2O_5 , M1 and M2 octahedra display the same compressibilities, with an average K of 225 GPa. Crystal compression of this disordered variant is less constrained along the a and c axes, and is thus more isotropic.

High pressure has been observed to induce ordering in many silicates (3, 14), including most of the major phases postulated for Earth's mantle (15). This pressure-induced ordering will affect EOS in two ways. First, the typically negative volume of ordering (2) will reduce room-pressure unit-cell volume, V_0 , of mantle phases equilibrated at high pressure; indeed, this negative ΔV_{dis} is the driving force for pressure-induced ordering. Second, ordering will itself affect elastic constants by subtle alteration of compression mechanisms, especially in cases of mixed-valence cation ordering, such as MgTi_2O_5 . We conclude that phases with significant ΔV_{dis} greater than 0.1%, including olivines, spinels, pyroxenes, carbonates, and feldspars (2), may also display EOS that are order-dependent.

EOS for geophysically relevant materials are usually made assuming rapid and reversible pressure-temperature-volume systematics. This assumption is invalid for phases that display order-disorder, because V_0 , compressibility, and presumably thermal expansivity are functions of the state of order. Given this situation, seismic velocities alone may be insufficient to resolve compositional effects from those of ordering in some minerals. Determination of EOS of minerals relevant to mantle conditions must thus be performed in situ, on crystals that have ordered states equilibrated with respect to both temperature and pressure.

REFERENCES AND NOTES

- S. P. Clark Jr., Ed., *Handbook of Physical Constants*, Geol. Soc. Am. Mem. **97** (1966); T. J. Ahrens, Ed., *Mineral Physics and Crystallography: A Handbook of Physical Constants*, Am. Geophys. Union Reference Shelf **2** (1995).
- R. M. Hazen and A. Navrotsky, *Am. Mineral.* **81**, 1021 (1996).
- T. Akamatsu, M. Kumazawa, N. Aikawa, H. Takei, *Phys. Chem. Miner.* **19**, 431 (1993).
- M. C. Domeneghetti, G. M. Molin, V. Tazzoli, *Am. Mineral.* **80**, 253 (1995); R. T. Downs, R. M. Hazen, L. W. Finger, *ibid.* **79**, 1042 (1994); G. Ottonello, A. Della Giusta, G. M. Molin, *ibid.* **74**, 411 (1989).
- C. H. Johansson and J. O. Linde, *Ann. Phys.* **25**, 1 (1936); K. Tsukimura, H. Nakazawa, T. Endo, O. Fukunaga, *Phys. Chem. Miner.* **19**, 203 (1992); H. S. T. O'Neill and W. A. Dollase, *ibid.* **20**, 541 (1994).
- R. M. Hazen, *Carnegie Inst. Washington Yearb.* **80**, 277 (1981).
- T. C. McCormick, R. M. Hazen, N. L. Ross, *Am. Mineral.* **74**, 1287 (1989).
- R. M. Hazen, J. Zhang, J. Ko, *Phys. Chem. Miner.* **17**, 416 (1990).
- R. M. Hazen, *Science* **259**, 206 (1993).
- _____, R. T. Downs, L. W. Finger, P. G. Conrad, T. Gasparik, *Phys. Chem. Miner.* **21**, 344 (1994).
- B. A. Wechsler and A. Navrotsky, *J. Solid State Chem.* **55**, 165 (1984); B. A. Wechsler and R. B. Von Dreele, *Acta Crystallogr.* **B45**, 542 (1989); N. E. Brown and A. Navrotsky, *Am. Mineral.* **74**, 902 (1989).
- O. L. Anderson and J. E. Nafe, *J. Geophys. Res.* **70**, 3951 (1965); D. L. Anderson and O. L. Anderson, *ibid.* **75**, 3494 (1970); R. M. Hazen and L. W. Finger, *ibid.* **84**, 6723 (1979).
- Unit-cell parameters and x-ray diffraction intensity data for four crystals were determined at 0.0, 1.03, 2.16, 3.22, 4.34, 6.20, and 7.51 GPa. Unit-cell parameters only were determined at 0.49, 1.68, 2.56, 3.84, 5.12, and 6.95 GPa.
- T. Akamatsu *et al.*, *Phys. Chem. Miner.* **16**, 105 (1988); R. M. Hazen, L. W. Finger, J. Ko, *Am. Mineral.* **77**, 217 (1992); *ibid.* **78**, 1336 (1993); R. M. Hazen, R. T. Downs, L. W. Finger, J. Ko, *ibid.*, p. 1320; R. M. Hazen, R. T. Downs, L. W. Finger, P. G. Conrad, T. Gasparik, *ibid.* **79**, 581 (1994).
- J. Ita and L. Stixrude, *J. Geophys. Res.* **97**, 6849 (1992).
- We thank N. Bector for help in preparation of the samples and C. T. Prewitt and D. Teter for useful discussions and constructive reviews. Crystal chemistry research at the Geophysical Laboratory was supported by NSF grant EAR9218845 and by the Carnegie Institution of Washington. High-pressure studies were supported in part by the NSF Center for High Pressure Research.

29 May 1997; accepted 20 August 1997

Implications of Satellite OH Observations for Middle Atmospheric H_2O and Ozone

M. E. Summers,* R. R. Conway, D. E. Siskind, M. H. Stevens, D. Offermann, M. Riese, P. Preusse, D. F. Strobel, J. M. Russell III

Satellite observations by the Middle Atmosphere High Resolution Spectrograph Investigation (MAHRSI) have produced global measurements of hydroxyl (OH) in the atmosphere. These observations reveal a sharp peak in OH density near an altitude of 65 to 70 km and are thus consistent with observations from the Halogen Occultation Experiment (HALOE) on the NASA Upper Atmosphere Research Satellite (UARS), which showed an unexplained H_2O layer at the same level. Analysis of stratopause (about 50 kilometers) OH measurements and coincident ozone observations from the Cryogenic Infrared Spectrometers and Telescopes for the Atmosphere (CRISTA) experiment reveals that the catalytic loss of ozone attributable to odd-hydrogen chemistry is less than that predicted with standard chemistry. Thus, the dominant portion of the ozone deficit problem in standard models is a consequence of overestimation of the OH density in the upper stratosphere and lower mesosphere.

The hydroxyl radical is arguably the single most important natural oxidizing agent in Earth's atmosphere (1), yet OH is very difficult to measure because of its high reactivity and thus its extremely low atmospheric abundance. In the middle atmosphere

(between ~15 and 90 km altitude), OH is known to play a fundamental role in the catalytic loss of atmospheric ozone (O_3) (2-4). Although previous ground-based and satellite platforms have produced extensive databases on middle atmospheric O_3 and H_2O (the parent molecule of OH), the MAHRSI and CRISTA observations have provided the first coincident observations of OH and O_3 at the stratopause (~50 km) and above (5, 6). In this region, the photochemistry of O_3 and odd hydrogen ($\text{H} + \text{OH} + \text{HO}_2$, denoted by HO_x) is thought to be relatively simple, whereas in the stratosphere HO_x chemistry is coupled to other catalytic cycles involving chlorine and ni-

M. E. Summers, R. R. Conway, D. E. Siskind, M. H. Stevens, E. O. Hulburt Center for Space Research, Naval Research Laboratory, Washington, DC 20375, USA.
D. Offermann, M. Riese, P. Preusse, Physics Department, University of Wuppertal, 42119 Wuppertal, Germany.
D. F. Strobel, Department of Earth and Planetary Sciences, Johns Hopkins University, Baltimore, MD 21218, USA.

J. M. Russell III, Department of Physics, Hampton University, Hampton, VA 23668, USA.

*To whom correspondence should be addressed.